

Developments towards an industrial Johnson noise thermometer

Paul Bramley, David Cruickshank^{id} and Jonny Aubrey

Metrosol Ltd, Plum Park Estate, Watling Street, Paulerspury, Northamptonshire NN12 6LQ, United Kingdom

E-mail: Paul.bramley@metrosol.co.uk

Received 9 August 2019, revised 15 October 2019

Accepted for publication 18 November 2019

Published 31 January 2020



Abstract

In this paper we present new developments in our practical, drift-free Johnson noise thermometer as it moves from a proof-of-principle prototype towards a practical implementation to become a viable primary thermometer for industrial applications. We will discuss bandwidth optimisation to obtain the lowest possible uncertainty of temperature measurements. The concept of weighting the cross-correlation frequency bins to improve the uncertainty will be introduced and it will be shown that this can decrease the measurement uncertainty in our system by 28%. Weighting fundamentally changes the optimum bandwidth calculation such that information from higher parts of the measured spectrum can always contribute to a reduction in total measurement noise. We will present the design approach used to provide extreme immunity to electromagnetic interference, a problem that has severely degraded previous efforts. We describe the results of tests by a third-party test laboratory demonstrating immunity up to field strengths of 10 Vm^{-1} , as required in standards for equipment operating in heavy industrial environments. We have also looked at interference at frequencies that could directly interfere with our thermometer that are not covered in the standards. The latest test results will be presented showing a five-fold improvement in accuracy on an extrapolation to absolute zero compared with the original proof-of-principle prototype with similar measurement parameters. Developments in techniques for providing traceability of the thermometer's calibration to electrical rather than temperature national standards will be presented.

Keywords: Johnson, primary, noise, thermometer, industrial

(Some figures may appear in colour only in the online journal)

1. Introduction

All industrial thermometers used today (such as thermocouples or PRTs), are 'secondary thermometers' in which a property that changes with temperature is measured. Measurements of this property are converted to a temperature reading using knowledge of the property to temperature characteristics determined by calibration. However, factors other than temperature (such as contamination of the thermometer materials, oxidation or transmutation) can affect the measured property, leading to calibration drift. In contrast, 'primary thermometers' measure a property that is linked

directly to thermodynamic temperature by a fundamental physical law, they therefore do not drift if the sensor becomes contaminated, oxidized or transmuted. Johnson noise thermometers (JNTs) are primary thermometers. A review of the wide variety of Johnson noise thermometry-based devices can be found in [1]. Note that many of them are not designed to be thermometers to measure temperature over a wide range. JNTs are based on the measurement of the small electrical noise signal (Johnson noise) generated by the thermally excited charge carriers in a resistive material and make use of the Johnson–Nyquist equation [2] relating noise to thermodynamic temperature:

$$V_n = \sqrt{4kTR \Delta f}. \quad (1)$$

Equation (1) can be re-arranged:

$$T = \frac{1}{4k} \left(\frac{V_n^2}{R \Delta f} \right). \quad (2)$$

Thermodynamic temperature (T) can therefore be determined by measuring the root mean squared (RMS) Johnson voltage noise (V_n), the sensor resistance (R), knowing the measurement bandwidth (Δf) and the Boltzmann constant ($k = 1.380649 \times 10^{-23} \text{ JK}^{-1}$ as recently set by international agreement [3]). These are all electrical measurements which can be made traceable to electrical rather than temperature standards. Note that with realisable circuits, Δf cannot be a simple rectangular bandwidth and equation (2) will need to be evaluated using spectral density, a summation of narrow individually calibrated bandwidths (the method used in the work presented here) or an integral to work out the effective bandwidth such as equation (9) from [1]:

$$\Delta f_c = \frac{\left[\int_0^\infty |G(f)|^2 df \right]^2}{\int_0^\infty |G(f)|^4 df}. \quad (3)$$

$G(f)$ is the frequency response of the system. In the work presented here, these electrical measurements are all made from the same short block of data. Throughout this paper, each individual temperature measurement is derived from a block of duration 6.5536 s. In this short time, the sensor cannot drift due to contamination, oxidation or transmutation as these are fundamentally slow processes. Other sources of drift, such as temperature changing cable capacitances or changes in amplifier gain, will not cause changes in readings as readings are based on the ratio of Johnson noise to calibration signal and these should both be equally effected. Significantly, the temperature determination is not affected by changes in any other property of the sensor, thereby making the measurement technique independent of any calibration and drift free. Of course, it is possible drift in the electronics used to measure the Johnson noise would lead to drift in the measurement, but with care modern electronics can make adequately stable measurements over years or even decades. Key to this stability is using a ratio-based system so amplifier gain is not a factor as this equally changes the Johnson noise and the calibration signal. Also, the frequency response of the vast majority of the measurement system used in this work is common to both the Johnson Noise signal and the calibration signal, so changes in this will not affect temperature readings based on their ratio. It is also a key point that the target accuracy is modest for an industrial system. It is limited by the statistical uncertainty of Rice's equation [4]:

$$\frac{\sigma_{V_n}}{V_n} = \frac{1}{\sqrt{\Delta f \Delta t}} \quad (4)$$

a fundamental equation that gives fractional standard deviation in terms of time and bandwidth. Note the fractional standard deviation is reduced by a larger bandwidth. In this equation σ_{V_n} is the standard deviation of the Johnson noise, V_n is the root

mean squared value of the Johnson noise as before and Δt is the integration time for the measurement. With the values used throughout this paper, $\Delta t = 6.5536 \text{ s}$, $\Delta f = 1.2 \text{ MHz}$, $T = 20 \text{ }^\circ\text{C}$ (293.15 K) and remembering that T is proportional to V_n^2 , equation (1), Rice's equation gives the lowest possible value of standard deviation of T as 0.209 K. This means that many effects such as the amplifier noise current [5] and amplifier nonlinearity [6] are negligible in comparison to the statistical uncertainty.

In the most advanced systems based on switching correlators employing quantum voltage standards [7], the effect of drift in the measurement electronics is eliminated if switching is sufficiently fast as well as generating a near perfect voltage reference signal. These systems are mostly employed at a single temperature, to either calculate the Boltzmann constant [8] or examine in detail fixed points [9, 10] and they can do this with low uncertainties. Although these switching correlators employing quantum voltage standards give low uncertainty, they use switching correlators that are dependent on matching the frequency responses of the two branches and using a frequency dependent correction. The frequency response match required, and the frequency dependent correction would change with temperature, so it is unclear how these systems could be adapted to measure a wide range of temperatures changing in real time. Also, we are looking at more industrial and practical thermometers so we cannot use the cryogenic systems employing quantum voltage standards and we must allow for changes in sense resistance and cable capacitance that will occur with measuring a wider range of temperatures. However, the industrial requirements for uncertainty are significantly more modest than those achieved by cryogenic switching correlators. Switching correlators are also inherently slower than ratio methods, see [1], section 5.3.1.

Over the years, numerous attempts have been made to produce working industrial JNTs [1, 11]. The principal application in recent years has been exploring discrepancies between the temperature scale (ITS-90) and thermodynamic temperature, or more recently determining the value for the Boltzmann constant for use in the recent redefinition of the Kelvin [12]. Despite efforts to develop practical JNTs for harsh industrial applications, where current technology does not provide adequate long-term stability (such as civil nuclear power generation [5]), there are currently no industrial thermometers based on Johnson noise.

Two significant problems frustrated prior attempts to produce a practical JNT; the limited bandwidth that could be used in the measurement (which leads to unacceptably long measurement times of minutes or hours) and inadequate immunity to external electromagnetic interference (EMI) [13]. In 2014, the authors started their development of a JNT using a new (patented) measurement technique that improves the bandwidth limitation. This is a ratio method where the temperature is calculated from the ratio of the Johnson noise to a calibration signal. A similar ratio method can be found in [14]. It is clear from equation (1) that increasing the bandwidth of a Johnson noise system will provide an increase in the received RMS voltage. It is also clear that if the system is limited by Rice's

equation (4), the standard deviation and uncertainty for a fixed temperature will decrease with an increase in bandwidth.

In the system described in this paper, the temperature is derived from the ratio of a current calibration signal to the Johnson noise, so the exact shape of the frequency response of the system is not important as long as it is the same for both the calibration signal and the Johnson noise. Increasing the bandwidth will only improve performance until the calibration signal starts to diverge in frequency response from the Johnson noise. This can happen due to a frequency response in the small part of the circuit that only effects the calibration signal, mostly the analogue part of the DAC and the feed-in resistor for the current calibration signal. Note that resistors in the system may have their own frequency response, the sensor resistance is common to both calibration and Johnson noise signal, however the current feed-in resistor is not. In practice, capacitance across the calibration current feed-in resistor is a problem and further work may look at a voltage-based calibration system.

This project started with the production of a proof-of-principal, benchtop prototype [15]. This provided temperature measurements with low enough uncertainty and enough accuracy for industrial applications in a few seconds. This paper describes our progress towards a practical industrial JNT, including improvements in performance, reduction in size and weight to a hand-held format. Significant work has been done on immunity to EMI and the device has been shown to achieve the high level of immunity required for ‘heavy industrial’ applications according to standards. We have also examined practical immunity at frequencies used directly within the device which could be more problematic with respect to interference.

2. Prior Art JNTs

The reader is referred to review papers [1] and [11] for an overview of the subject. There are two significant challenges when realizing a JNT; measuring the very small signal levels (V_n) involved and determining or allowing for the frequency response of the system ($G(f)$).

The Johnson noise signal is at the limit of measurement. Any amplifiers used in the measurement system adds noise that is comparable to the Johnson noise being measured. The best solution is to connect the sensor to two similar low-noise amplifiers and then use a correlator to suppress noise and extract the Johnson noise signal. Correlators can be either time domain [16] (figure 1) in which the signal from the two amplifiers is simply multiplied together before passing through a low-pass filter (often an integrator) [8, 16, 17]. Alternatively, the correlator can work in the frequency domain, where the digitized output from each amplifier are converted to the frequency domain using a fast Fourier transform (FFT). The FFT bin for each frequency interval is then multiplied by the complex conjugate of the corresponding bin from the other

amplifier before being summed over the measurement bandwidth [18, 19] (figure 2).

Equation [1] lends itself to an ideal rectangular filter but is impossible to produce a filter (either analogue or digital) with a flat frequency response and a hard cut-off frequency, such a filter is non-causal. If a filter’s response is not rectangular in the frequency domain, this makes it difficult to determine the measurement bandwidth to be used in equation [1]. This together with the need to know the sensitivity of the measurement electronics means that prior art JNTs use a substitution technique and switch between measuring the Johnson noise signal and a known ‘white’ (equal power at all frequencies of interest) calibration signal. This can simply be a known value resistor at a known temperature as shown in figure 1 or a synthetic calibration signal. The ratio of these two measurements and knowledge of the power spectral density of the calibration signal allows the JNT system to measure an absolute noise spectral power density and therefore a temperature determination see [1] section 3.2. Very often the frequency response of the two branches is adjusted to be matched by trimming, usually adding capacitance to one branch so the RC time constant of the two branches matches. In this case, the frequency response of the two branches cancels out of the ratio. For better performance, a residual spectral mismatch error is calculated and corrected for. These switching correlator systems separate the Johnson noise and calibration signals by switching in the time domain (figure 1).

This time domain switching approach creates a serious problem for thermometers designed to work over a range of temperatures. In order for the system to work, the system bandwidth must remain the same as it switches between measuring the Johnson noise and the calibration signal. At fixed sensor temperatures this can be achieved by matching the cable’s capacitance by trimming and modeling the residual error. This works well with systems that operate at a fixed temperature and where the cable capacitance and the sensor resistance are not expected to change with time. In devices operating over a range of temperatures, in an otherwise harsh environment or over a long period of time, the frequency response of the sensor branch will inevitably change with time. This will be largely due to the transmission lines (cables) combining with the sensor resistor having a changing frequency response (primarily due to the cable capacitance and sensor resistance changing with temperature) [21]. In these time varying scenarios, a fixed trimming and modeling of the residual error will not work. In these circumstances, the drift-free advantage of JNT is lost, as the result has become dependent on the resistance of the sensor and the cable capacitance. By using only low frequencies, well below the cut-off frequency of the cable and sensor system, this sensitivity can be minimized. But, in any practical system involving even 0.5 m of cable from the sensor to the input amplifiers, this restricts the sensor resistance and bandwidth to about 100 Ω and 100 kHz. This in turn limits the available Johnson noise signal and necessitates

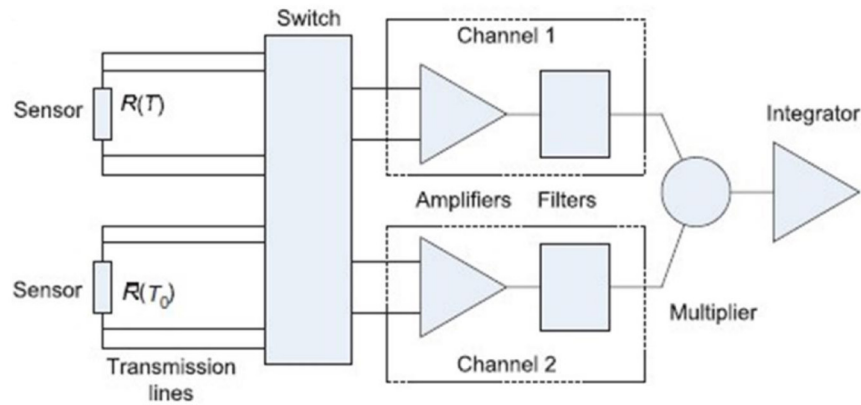


Figure 1. JNT System using a time domain correlator and a known resistor at a known temperature $R(T_0)$ as a reference. Reproduced from [20]. © 2012 BIPM & IOP Publishing Ltd.

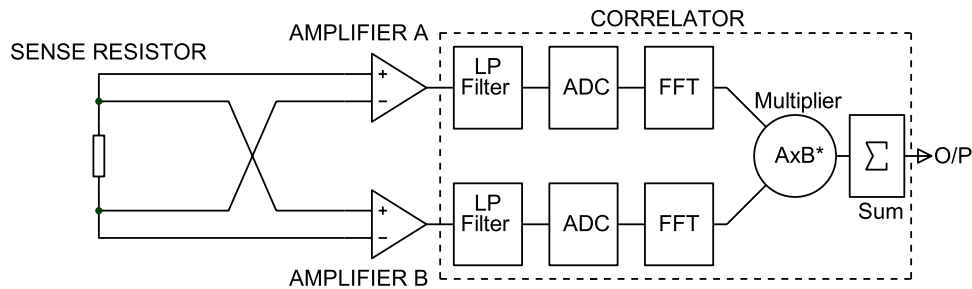


Figure 2. JNT system using a frequency domain correlator. LP = low pass, ADC = analogue to digital converter, FFT = fast Fourier transform [18].

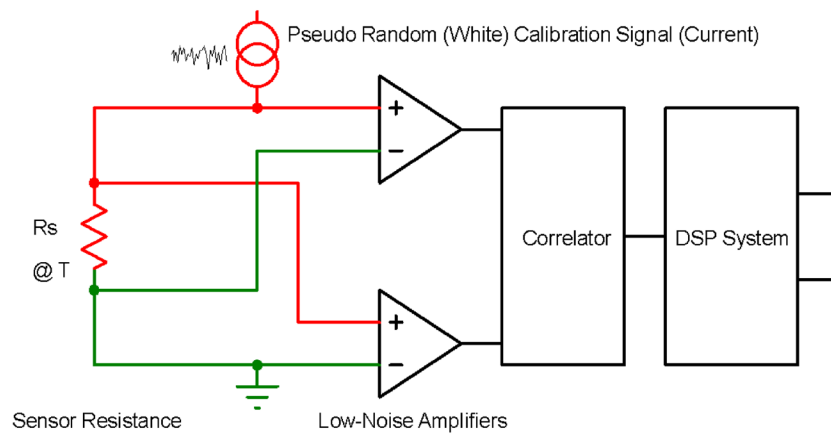


Figure 3. New JNT technique using pseudo random current injection which can be separated from Johnson noise in the frequency domain.

integration times of many minutes or even hours in order to achieve the required uncertainty for industrial applications. This is too slow for most industrial applications.

3. New JNT topology

The new topology devised by the authors allows the Johnson noise signal and the calibration signal to be separated in the frequency domain. This means that frequencies up to and well beyond the corner frequency created by the sensor resistance and input cable capacitance can be used as well as a much higher sense resistance. Higher frequencies lead to a larger bandwidth, which gives more signal power, equation (1), and

a lower fractional standard deviation equation (4). The effect is to increase the Johnson noise signal by several orders of magnitude, thereby allowing temperature measurements to industrial uncertainty levels to be made in acceptable response times (a few seconds). This new arrangement involves producing a ‘white’, pseudo random noise (PRN) current for the calibration signal and injecting this directly into the measurement system (figure 3). Other methods of injection could include capacitive or inductive coupling [14, 18]. The PRN signal comprises a comb of harmonically related tones, each one exactly centered in an FFT bin (to prevent signal leakage into adjacent bins) with randomized phase. These tones appear in only some of the bins (figure 4) [14, 22].

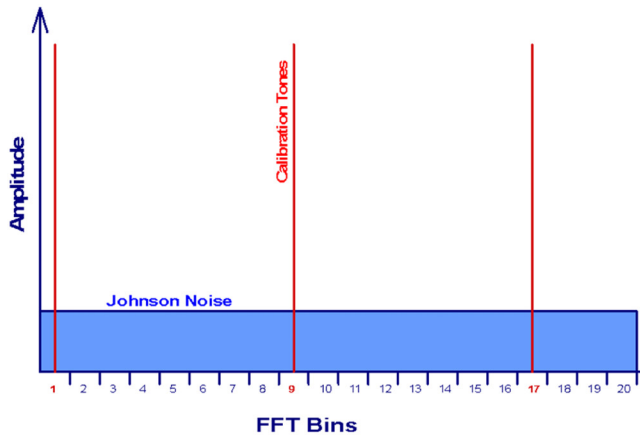


Figure 4. Pseudo-random noise current calibration signal (frequency domain).

This allows the calibration signal to be separate from the Johnson noise signal using frequency domain multiplexing; the Johnson noise power can be determined by summing the power in the bins that do not have a tone signal in them. The calibration signal can then be determined by measuring the power in bins that do have a tone in them and then subtracting, in quadrature, the Johnson noise power already calculated [15].

In practice care must be taken that the calibration tones have a known frequency response when combined with the Johnson noise we are trying to measure. It is simplest if this is a flat white response, the same power at all tones. This means the DAC source of the tones and the feed in circuitry would need to have a combined flat response. If any part of this circuitry does not have a flat response, if the response is fixed, this can be allowed for in the files feeding the DAC. If it varies with time it can be measured at the DAC output providing a suitable measurement sub system can be designed.

At the receiver any frequency response of the ADC system will equally change the calibration and the Johnson noise signals and therefore will not change the ratio. There could be some second order effects at the edges of the received bands but for the industrial accuracy sought these are negligible.

One downside of the system proposed here is that it is not possible to inject the calibration signal at the point you would really want to, at the sensor. It is possible to inject our calibration signal at one of the amplifiers and this is very close to the equivalent of injecting it at the sense resistor, even considering the frequency response of the cables, see [15], section 3.1.

However, this means for precision measurements a switching correlator that is not subject to this error may be more suitable.

Note that all Johnson noise thermometers are limited by Rice's equation (4) but the system proposed in this paper does not involve two noisy measurements taken at separate times as required in the case of a switching correlator, this gives distinct advantages in measurement time, see section 5.3.1 in [1].

Lower amplitude problems, such as nonlinearity in DACs, ADCs and amplifiers will be completely masked by the statistical uncertainty in Rice's equation for an industrial target accuracy of between 0.1 and 1 K.

In comparison with a switching correlator, a JNT of this architecture can adjust for changes in the frequency response



Figure 5. Original proof-of-principle prototype.

of the system caused by temperature fluctuations relatively quickly, there is no need to rebalance the frequency response of the two arms or calculate a new model for the residual errors. It measures the resistance of the sensor and the frequency response from the same data block as the temperature is determined. Throughout this paper the blocks used were 6.553 s in duration for each temperature measurement.

4. Reduction in size and weight

The original proof-of-principle prototype weighed 35 kg and had a volume of 70 l (figure 5). It used commercial off-the-shelf (COTS) instruments to perform many of the functions, such as digitizing the amplified noise waveforms (using an Agilent L4532A digitizer) and generating the pseudo-random noise waveforms (using an Agilent Trueform 33500B series waveform generator).

We are systematically replacing all the COTS instruments with dedicated bespoke electronics. This allows us to optimize performance for this specific application thereby improving performance as well as reducing size. For example, the original prototype used a dual channel, 16-bit data acquisition instrument made by Agilent Technology, which has been replaced by our own 24-bit ADC system giving a significant reduction in size and power consumption and improvement in performance (see table 1).

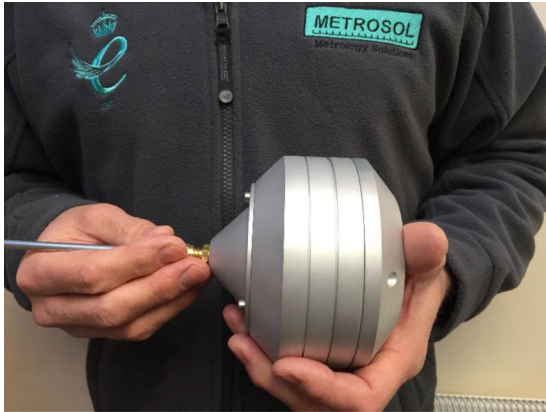
Significant progress has been made towards the project target of reducing the weight and size of the system to <1 kg and <1 l (figure 6). At present, some of the electronics remains outside the main enclosure and still use COTS instruments, but by the end of the project the entire signal processing system will be integrated into the main enclosure with an ethernet or USB interface.

5. Results: measurement performance

Figure 7 shows initial results from the new prototype. This shows measured Johnson noise power from our Johnson noise prototype 2 plotted against the temperature of an oil bath it was immersed in. This prototype uses a cross correlator

Table 1. Improvements in ADC with JNT2 Prototype.

Parameter	COTS based JNT	New JNT2 system
Resolution	16 bit	24 bit
Sample rate	20 MS s ⁻¹	20 MS s ⁻¹
Effective number of bits (ENOB)	12	17
Temperature coefficient	0.02 % K ⁻¹	0.0002 % K ⁻¹
Drift (1 year)	0.04%	0.006%
Power consumption	45 W	3.3 W
Volume	6970 cm ³	16 cm ³

**Figure 6.** New JNT2 prototype showing a significant reduction in weight and volume from the proof of principle prototype shown in figure 5.

between two amplifier chains to all but eliminate the effect of amplifier noise. The vertical axis is an arbitrary (uncalibrated) power from the cross correlator. The important feature in this graph is that at zero power the projection of a straight line fit to the measurement points gives an intercept at -273.415 °C. This should be absolute zero, -273.15 °C. This is a significant improvement (over 5 times less error) over the proof of principal prototype which had this intercept at -271.79 °C. The standard deviation of the difference between the measured points and the least square linear fit trendline to the data $y = 8.9243365009 \times 10^3 \times +2.3662114268 \times 10^3$ is $\sigma = 0.017652$ K. This means even allowing for the long projection back to 0K the improvement in the intercept at 0K is statistically significant.

6. Immunity to electromagnetic fields

Previous efforts to produce a practical JNT have all encountered unresolved problems caused by inadequate immunity to external EMI. Some have tried to mitigate the problem by using signal processing to remove any interference from the signal [5, 7], but this approach is fundamentally flawed since the interfering noise parameters are unknown and can be indistinguishable from real noise thereby causing measurement errors. The authors have taken the view that the only safe way to deal with EMI is to ensure that it does not get into the measurement signal in the first place. The new prototype therefore uses the design strategy proposed for coaxial AC bridges by Kibble and Rayner [8]. The new prototype follows

full coaxial theory where a coaxial cable that has an equal but opposite current in its core and screen produces no electrical or magnetic field outside the cable and therefore is not susceptible to an electrical or magnetic field outside the cable. This is a more effective approach than considering a coaxial cable as merely a screened core. An early version of the new prototype (in which all the front-end amplifiers were inside the JNT enclosure, but the ADC was still a COTS instrument) was taken to an accredited EMC test laboratory (figure 8). There it was tested for immunity to electromagnetic radiation in accordance with EN61000-4-3 [23] (at 10 V m⁻¹ from 80 to 1000 MHz, 3 V m⁻¹ from 1.0 to 2.7 GHz). This is the most extreme ‘heavy Industrial’ level of immunity under the standard and the highest the laboratory could generate.

The new JNT prototype proved to be completely immune to the applied fields, making it the first JNT to be capable of working in real world, extreme electromagnetic environments to official standards. While immunity to interference from the radiated waves in EN61000-4-3 is important in terms of compliance, in practice the JNT could be susceptible to interference at frequencies it uses directly, 10kHz to 1.2 MHz. Early versions of this JNT did occasionally show some interference that could be related to AM radio stations for example but since the full EMC package with coaxial and triaxial design was introduced, no interference has been observed over an extended period of time and in a wide variety of locations within our laboratories and at sites nationally and internationally. This is illustrated in figure 9, where the spectrum is entirely smooth. This is regularly checked during experiments. We have also tried some more extreme tests, like placing the probe near the electron beam deflection circuitry on a cathode ray tube computer monitor. Only by placing the probe against the case of the monitor near the deflection circuitry was any interference observed. A more scientific and quantified test will be carried out in the future with a more final version of the JNT.

7. Improved signal processing

Prior art JNTs typically use around 100 Ω as the sense resistance and it is unclear what bandwidth they would be able to use and still be able mitigate the effects of frequency response changes during switching between the DUT and calibration signals, especially over a wide range of temperatures. In such systems, the signals in each FFT bin are similar and simply summing up the bins to integrate the signal is adequate. However, in our system we use a much higher sense resistance (typically 5 k Ω) to increase the available Johnson noise signal and minimise systematic errors in the measurement due to the asymmetry of the current injection [15]. Other errors due to preamplifier limitations are discussed in [5], but these are small compared with the error from the statistical uncertainty from Rice’s equation (4). Noise from the feed-in resistor of the current source may also be significant even after attenuation by the potential divider formed by it and the sensor, if it is it can be calculated and deducted (in quadrature) from the measured noise. Current noise from the amplifiers will be

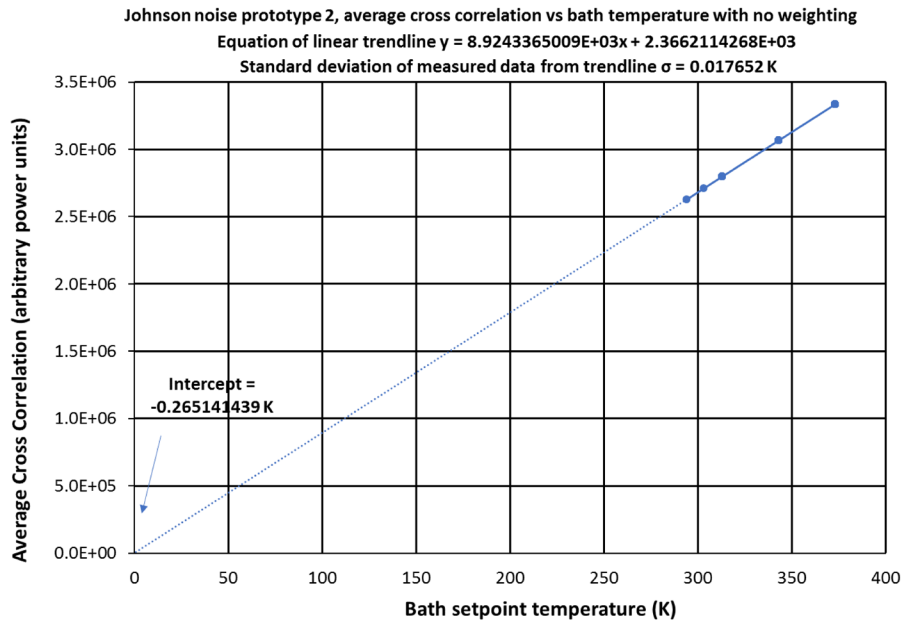


Figure 7. Measured Johnson noise power from our Johnson noise prototype 2 versus the temperature of an oil bath it was immersed in.

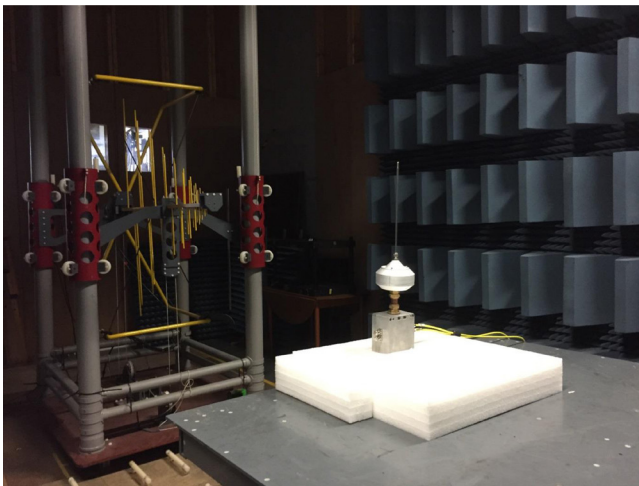


Figure 8. EMC Tests on the new JNT prototype.

turned into voltage noise by the sensor resistor. This noise is correlated at both amplifiers. However, by using JFET amplifiers this noise is measured in fA (the amplifiers used for all work here have a current noise of $0.6 \text{ fA } \sqrt{\text{Hz}}^{-1}$ at a frequency of 10 kHz therefore even with a $5 \text{ K}\Omega$ sense resistor it will be insignificant compared with the statistical noise). We also use a much higher bandwidth (1.2 MHz) to increase the Johnson noise signal measured, but this means that the signal power in each FFT bin reduces significantly at higher frequencies (figure 9) as this high resistance combines with the cable capacitance to lower the cut-off frequency of the low pass RC filter.

The effect of this is that the uncertainty arising from the amplifier noise increases with frequency as can be seen if we take the ratio of the Johnson noise to the calibration tones localized to each frequency tone as shown in figure 10.

The average ratio of JN to calibration power is the same at all frequencies (white) as expected, but the uncertainty

(scatter) increases with frequency as the relative residual amplifier noise after the correlator increases with diminishing Johnson noise signal. This is caused by the probe (the cable capacitance combined with the sense resistor) acting as a low pass filter. If we simply sum up the FFT bins to provide a measurement of the total Johnson noise and use this to determine temperature then at some point the additional, degraded data at high frequency will increase rather than decrease the total measurement uncertainty, even though the additional data does contain useful information on the Johnson noise. This can be seen if we sum noise over different bandwidths and then calculate the standard deviation of the resulting temperature for these determinations (Unweighted trace in figure 11).

Measurements were taken by immersing the probe in an oil bath controlled to $20 \text{ }^\circ\text{C}$. The standard deviation is the 1σ uncertainty. Beyond about 400 kHz, adding further data (increasing the bandwidth) increases rather than decreases the uncertainty of the temperature measurement for unweighted data.

More careful consideration of the data, specifically weighting the data, can ensure that adding the additional high frequency data always improves the final measurement uncertainty. If we consider how best to combine two Johnson noise power ratio measurements (P_1 and P_2) made at two different frequencies, they will show the same average value P but may have different uncertainties U_1 and U_2 due to amplifier noise that has not been removed by the correlator. A weighted average (P_W) of the two values will be

$$P_W = x_1 P_1 + x_2 P_2 \quad \text{where} \quad x_1 + x_2 = 1.$$

Therefore $P_W = x_1 P_1 + (1 - x_1) P_2$

The amplifier voltage noise after correlation is substantially uncorrelated between the two amplifiers. Any amplifier current noise will generate a noise signal that is common to

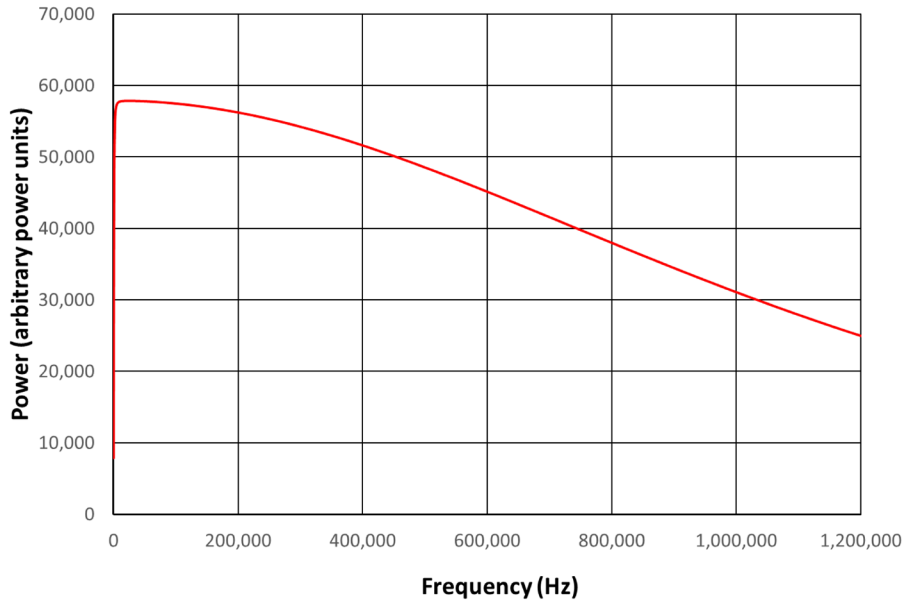


Figure 9. Variation of Johnson noise power with frequency.

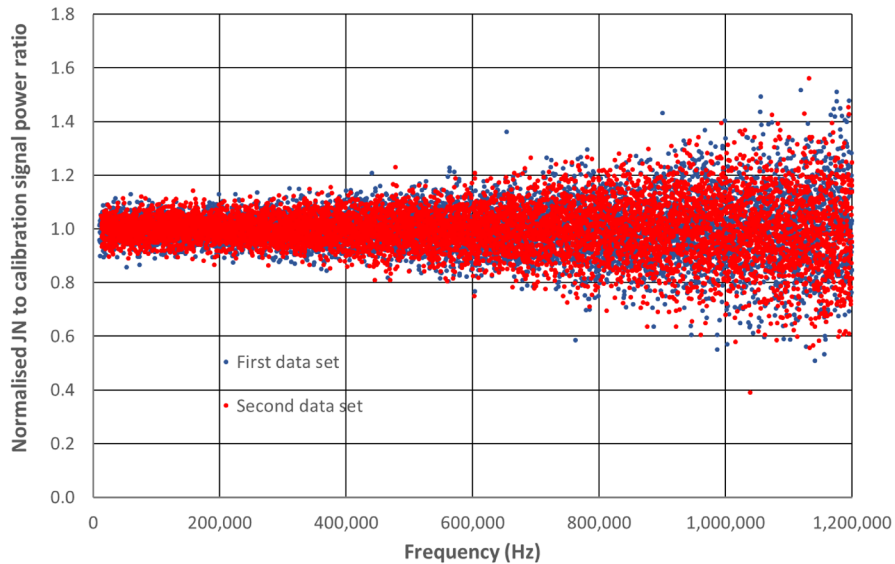


Figure 10. Increase in scatter of normalized ratio of JN to calibration tone power with frequency.

both channels, but we use FET input stages to the amplifiers so that this noise source is negligibly small. As a result, the uncertainty on the weighted average (U_A) will be

$$U_A = \sqrt{x_1^2 U_1^2 + (1 - x_1)^2 U_2^2}. \quad (6)$$

Differentiating equation (6): this uncertainty will be a minimum when

$$\frac{dU_A}{dx_1} = \frac{1}{2} \frac{1}{\sqrt{x_1^2 U_1^2 + (1 - x_1)^2 U_2^2}} [2x_1 U_1^2 - 2U_2^2 + 2x_1^2 U_2^2] = 0.$$

This occurs when

$$x_1 (U_1^2 + U_2^2) = U_2^2.$$

This can be more usefully expressed as

$$x_1 = \frac{1}{U_1^{-2} + U_2^{-2}} \quad (7)$$

$$x_2 = \frac{1}{U_2^{-2} + U_1^{-2}}. \quad (8)$$

This indicates that the minimum uncertainty is achieved when combining two measurement if we weight the data in proportion to the inverse of the uncertainty squared. The common bracket term is there to renormalize the result to become the average.

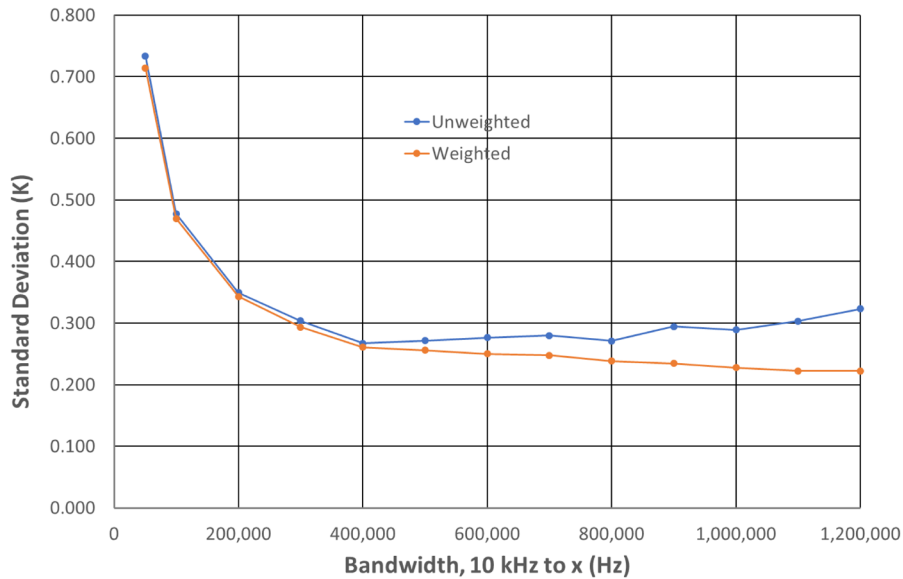


Figure 11. Standard deviation of 6.5536 s samples versus bandwidth (10kHz to value shown on x-axis).

The minimum uncertainty (substituting equations (7) and (8) into (6)) is then

$$U_{Amin} = [U_1^{-2} + U_2^{-2}]^{-1} \sqrt{\left(\frac{1}{U_1^2}\right)^2 U_1^2 + \left(\frac{1}{U_2^2}\right)^2 U_2^2} = [U_1^{-2} + U_2^{-2}]^{-1/2}. \tag{9}$$

With more data points, it is evident that they should all be weighted in proportion to the inverse of their squared uncertainties in order to provide the best (lowest uncertainty) result. This can be seen if we consider adding a third point P_3 , having uncertainty U_3 and weight it by x_3 , from analogy with equation (7) we see that the minimum uncertainty is achieved when

$$x_3 = \frac{1}{U_3^2} [U_3^{-2} + U_{Amin}^{-2}]^{-1}.$$

Substituting in U_{Amin} from equation (9), we get

$$x_3 = \frac{1}{U_3^2} [U_3^{-2} + U_{Amin}^{-2}]^{-1} = \frac{1}{U_3^2} [U_3^{-2} + U_1^{-2} + U_2^{-2}].$$

The general form and the one used in our system is that the power ratio measurements from the FFT bins are combined by weighting to determine an optimal measurement P_O as follows:

$$P_o = \frac{\sum_{y=1}^{y=N} \frac{1}{U_y^2} P_y}{\sum_{y=1}^{y=N} \frac{1}{U_y^2}}.$$

By weighting the data from the FFT bins before combining them, the additional data from the higher frequency higher uncertainty data always improves the overall measurement uncertainty as seen in the Weighted trace in figure 11 where the fractional standard deviation at 1.2 MHz bandwidth reduces from 0.323 K to 0.232 K (a 28% improvement).

There is however diminishing returns. The desired Johnson noise signal is attenuated by the low pass filter formed by the

sense resistor and the cable capacitance. Therefore, further increases in system bandwidth will only give modest further reductions in fractional standard deviation and uncertainty as the Johnson noise becomes close to or even below the power of the residual amplifier noise or the numerical noise in the processing. Further work needs to be done to determine the ultimate limiting factor. This type of system strongly favors short cables with low capacitance.

8. Conclusions

We have discussed in detail a new prototype Johnson noise thermometer where measurements are made with respect to electrical rather than temperature standards. We have shown that when taking power measurements over a range of temperatures and then projecting the reading back to zero power, the intercept with the temperature axis is -273.415°C , very close to absolute zero, -273.15°C . We have shown that summing measurements across frequencies without weighting leads to an optimal bandwidth to sum to, summing any further degrades the uncertainty. If we weight the summation according to the inverse of the squared uncertainty at each frequency, there is no optimum bandwidth, the larger the bandwidth the better. For the system studied this weighting process produced a 28% reduction in uncertainty compared with the unweighted case. We have discussed the key coaxial principal of connection with regard to EMC and shown that careful following of this principal can lead to immunity from EMI at heavy industrial levels according to standards and in scenarios which are more likely to cause interference in practice.

ORCID iDs

David Cruickshank  <https://orcid.org/0000-0002-5477-8497>

References

- [1] Qu J F, Benz S P, Rogalla H, Tew W L, White D R and Zhou K L 2019 Johnson noise thermometry *Meas. Sci. Technol.* **30** 1–26
- [2] Nyquist H 1928 Thermal agitation of electric charge in conductors *Phys. Rev.* **32** 110–3
- [3] Newall D B *et al* 2018 The CODATA 2017 values of h , e , k and N_A for the revision of the SI *Metrologia* **55** L13–6
- [4] Rice S O 1944 Mathematical analysis of random noise *Bell Syst. Tech. J.* **23** 282–332
- [5] White D R and Zimmermann E 2003 Preamplifier limitations on the accuracy of Johnson noise thermometers *Metrologia* **37** 11–23
- [6] Qu J, Benz S P, Rogella H and White D R 2009 Reduced non-linearities and improved temperature measurements for the NIST Johnson noise thermometer *Metrologia* **46** 512–24
- [7] Nam S W, Benz S P, Dresselhaus P D, Tew W, White D R and Martinis J M 2003 Johnson noise thermometry measurements using a quantized voltage noise source for calibration *IEEE Trans. Instrum. Meas.* **52** 550–4
- [8] Flowers-Jacobs N E, Pallarolo A, Coakley K J, Fox A E, Rogalla H, Tew W L and Benz S P 2017 A Boltzmann constant determination based on Johnson noise thermometry *Metrologia* **54** 730–7
- [9] Tew W, Benz S P, Dresselhaus P D, Coakley K J, Rogalla H, White D R and Labenski J R 2010 Progress in noise thermometry at 505 K and 693 K using quantized voltage noise ratio spectra *Int. J. Thermophys.* **31** 1–31
- [10] Edler F, Kuhne M and Tegeler E 2003 Noise temperature measurements for the determination of the thermodynamic temperature of the melting point of palladium *Metrologia* **41** 47–55
- [11] White D R *et al* 2003 The status of Johnson noise thermometry *Metrologia* **33** 325–35
- [12] de Podesta M 2016 Rethinking the Kelvin *Nat. Phys.* **12** 104
- [13] White D and Mason R 2004 An EMI test for Johnson noise thermometry *Proc. TEMPMEKO (Zagreb)*
- [14] Callegaro L, D’Elia V, Pisani M and Pollarolo A 2009 A Johnson noise thermometer with traceability to electrical standards *Metrologia* **46** 409–15
- [15] Bramley P, Cruickshank D and Pearce J 2017 The development of a practical, drift-free, Johnson-noise thermometer for industrial applications *Int. J. Thermophys.* **38**
- [16] Brixy H and Kakuta T 1996 Noise thermometer *Japan. At. Energy Res. Inst. Rev.* **96-003** (<https://www.osti.gov/etdweb/servlets/purl/368199>)
- [17] Crossno J, Liu X, Ohki T A, Kim P and Fong K C 2014 Development of high frequency and wide bandwidth Johnson noise thermometry *Appl. Phys. Lett.* **106** 023121
- [18] Kisner R A, Britton C L, Jagadish U, Holcomb D E, Bobrek O, Roberts M J, Hwang I K, Moon B S, Miller D W and Talmagi J W 2005 Development of a Johnson noise thermometer for nuclear power use *Final Project Report Subtask 2.2 of International Nuclear Energy Research Initiative*
- [19] Bull N D 2016 An innovative approach to Johnson noise thermometry by means of spectral estimation *PhD Dissertation* University of Tennessee (https://trace.tennessee.edu/utk_graddiss/3897)
- [20] White D R 2012 Non-linearity in Johnson noise thermometry *Metrologia* **49** 651–65
- [21] White D R and Qu J 2017 Frequency-response mismatch effects in Johnson noise thermometry *Metrologia* **55** 38
- [22] White D R and Benz S P 2008 Constraints on a synthetic noise source for Johnson noise thermometry *Metrologia* **45** 93–101
- [23] IEC EN 61000-4-3 2006 *Electromagnetic Compatibility—Part 4-3: Testing and Measurement Techniques—Radiated, Radio-Frequency, Electromagnetic Field Immunity Test* (International Electrotechnical Commission)